NeuroImage 87 (2014) 383–394

Contents lists available at ScienceDirect

NeuroImage

journal homepage: www.elsevier.com/locate/ynimg

How delays matter in an oscillatory whole-brain spiking-neuron network model for MEG alpha-rhythms at rest

Tristan T. Nakagawa [a,*], Mark Woolrich [b], Henry Luckhoo [b], Morten Joensson [c,d], Hamid Mohseni [b], Morten L. Kringelbach [c,d], Viktor Jirsa [e], Gustavo Deco [a,f]

[a] Center for Brain and Cognition, Computational Neuroscience Group, Department of Information and Communication Technologies, Universitat Pompeu Fabra, Barcelona 08018, Spain
[b] Oxford Ctr. For Human Brain Activity, Univ. of Oxford, Oxford, United Kingdom
[c] Department of Psychiatry, University of Oxford, Oxford, UK
[d] Center of Functionally Integrative Neuroscience (CFIN), Aarhus University, Denmark
[e] Institut de Neurosciences des Systèmes UMR INSERM 1106, Aix-Marseille Universitè, 13005 Marseille, France
[f] Institució Catalana de la Recerca i Estudis Avançats, Universitat Pompeu Fabra, Barcelona 08010, Spain

ARTICLE INFO

Article history:
Accepted 5 November 2013
Available online 16 November 2013

Keywords:
Resting-state model
MEG
Delays
Spontaneous alpha
Alpha-oscillations
SFA
Spike-frequency adaptation

ABSTRACT

In recent years the study of the intrinsic brain dynamics in a relaxed awake state in the absence of any specific task has gained increasing attention, as spontaneous neural activity has been found to be highly structured at a large scale. This so called resting-state activity has been found to be comprised by nonrandom spatiotemporal patterns and fluctuations, and several Resting-State Networks (RSN) have been found in BOLD-fMRI as well as in MEG signal power envelope correlations. The underlying anatomical connectivity structure between areas of the brain has been identified as being a key to the observed functional network connectivity, but the mechanisms behind this are still underdetermined. Theoretical large-scale brain models for fMRI data have corroborated the importance of the connectome in shaping network dynamics, while the importance of delays and noise differ between studies and depend on the models' specific dynamics. In the current study, we present a spiking neuron network model that is able to produce noisy, distributed alpha-oscillations, matching the power peak in the spectrum of group resting-state MEG recordings. We studied how well the model captured the inter-node correlation structure of the alpha-band power envelopes for different delays between brain areas, and found that the model performs best for propagation delays inside the physiological range (5–10 m/s). Delays also shift the transition from noisy to bursting oscillations to higher global coupling values in the model. Thus, in contrast to the asynchronous fMRI state, delays are important to consider in the presence of oscillation.

Introduction

It is an astonishingly hard task to do, think, and attend nothing; thoughts, observations, and feelings naturally arise from within us, more or less at random. Without any specific external stimulation, we fluctuate in our mental states as the brain fluctuates between different activity patterns. While in the study of cognitive tasks, these fluctuations seem to be a nuisance that necessitate averaging over many trials, they are themselves structured and informative in many ways. fMRI and, more recently, neurophysiological imaging studies have found that the brain's spontaneous activity patterns decompose into networks of brain areas, defined primarily not by their mean activity level but by the functional connectivity between them (Mazoyer et al., 2001). This way, several Resting-State Networks (RSN) with known task-related functional importance such as sensorimotor, visual and attentional areas and networks, have been identified in spontaneous brain activity in the absence of tasks (Biswal et al., 1995, 1997; Cordes et al., 2000, 2002; Damoiseaux et al., 2006; De Luca et al., 2005, 2006; Lowe et al., 1998). A specific 'Default Mode Network' (Buckner et al., 2008; Damoiseaux et al., 2006; Greicius et al., 2003; Gusnard and Raichle, 2001; van den Heuvel et al., 2008), an RSN which shows higher activity during the resting-state than during various task conditions, has also been identified. These functional networks and their dynamics are determined both by the underlying anatomical connectivity and the local neuronal dynamics and interactions, leading to spatiotemporal patterns and oscillations at different time scales. To understand them is of key value to understanding the brain's cognitive machinery and its ability to flexibly control mental states. So, it is of prime interest to gain deeper insight into the origins and mechanisms of spontaneous functional connectivity (FC) patterns, and we can apply theoretical models and numerical simulations of resting-state activity to study these dynamics.

* Corresponding author.
E-mail address: tristan.nakagawa@upf.edu (T.T. Nakagawa).

1053-8119
http://dx.doi.org/10.1016/j.neuroimage.2013.11.009

Resting-state models take advantage of recent technical advances capable of tracking white fiber tracts noninvasively via DTI/DSI in humans (Cabral et al., 2011; Deco and Jirsa, 2012; Honey et al., 2009, 2010; Izhikevich and Edelman, 2008; Senden et al., 2012) to combine realistic neuroanatomical long-range connections between brain areas with the models' local dynamics (oscillators, neural masses, or explicitly modeled neurons) in order to construct a dynamical cortical model for the human cortex. The simulated activity patterns from the freely interacting network have successfully reproduced resting-state dynamics: Anticorrelated functional networks such as found by Fox et al. (2005) in cortex have been observed to emerge in models with different local dynamics (e.g. Honey et al., 2007: chaotic oscillators; Deco et al., 2009: Wilson–Cowan oscillators). Slow fMRI rhythms below 1 Hz observed by several authors in fMRI resting-state recordings (Biswal et al., 1995; Cordes et al., 2001; Damoiseaux et al., 2006; De Luca et al., 2006; Fransson, 2005) can also be found in Wilson–Cowan (Deco et al., 2009), Kuramoto oscillator (Cabral et al., 2011), neural mass (Honey et al., 2007), and spiking neuron models (Deco and Jirsa, 2012). In all these models, the underlying network structure is crucial in shaping the network dynamics and maintaining the system close to criticality (see Deco et al., 2013a, 2013b). Further, delays were found to shape the emerging spatial patterns and modes in oscillatory networks much more in directed graphs (Ghosh et al., 2008a,b) than in undirected graphs (Knock et al., 2009). In general, the extent to which delays (and noise) critically influence the global dynamics and interactions, depends also on the nature of local network dynamics (Deco and Corbetta, 2011; Deco et al., 2009). Consequently, the choice of local dynamics depends on various factors and goals that are pursued by the studies, as for example, the desired level of abstraction/physiological realism, the time- and spatial scales, and the network mechanisms to be investigated.

While modeling studies have so far been mostly focused on fMRI FC and slow oscillations that were empirically observed, recent neurophysiological studies have investigated the resting-state with increasing temporal resolution. Using combined EEG/fMRI and source-reconstructed MEG recordings to increase spatial resolution, these studies have found that alpha and beta band-limited power (BLP) envelopes retrace fMRI based FC patterns and slow fMRI rhythms (Brookes et al., 2011a, 2011b; de Pasquale et al., 2010; Hipp et al., 2012; Liu et al., 2010; Mantini et al., 2007). So far, the various anatomically informed, oscillatory dynamics network models have been limited to fMRI, and have not yet been validated with empirical neurophysiological data, which can capture faster oscillations. In MEG recordings, for example, alpha-oscillations are especially predominant in, and have always been associated with the resting-state. They are readily identifiable and robustly found in electrophysiological recordings since the first human EEG studies by Hans Berger a century ago (for a historical overview, see Shaw, 2003). The origin of this typical alpha-activity is not comprehensively determined yet, though self-sustaining sources have been identified both in cortex (Silva et al., 1991) and in the thalamocortical loop (Lopes da Silva et al., 1974). In fact, alpha-activity is most likely a collection of rhythms from several sources (Ben-Simon et al., 2008; Freyer et al., 2011; Neymotin et al., 2011; Shaw, 2003), which may contribute to the variability of alpha-rhythm characteristics (e.g. peak frequency, amplitude, topography) found in the brain both over time (Freyer et al., 2009, 2011, 2012) and between subjects (Chiang et al., 2011).

In the present study, we focused on the influence of noisy oscillations on band-limited connectivity patterns in a biophysical setting. As the integrity of a model always depends on the spatial connectivity structure, but not in all cases on the temporal structure (e.g. in the case of chaotic oscillators, Honey et al., 2007, 2009; or in the asynchronous state (Deco and Jirsa, 2012)), it is unclear to what extent the brain's effective connectivity is affected by, and sensitive to the delays introduced by long fibers and limited transmission velocities in the brain, when considering complex neuronal population dynamics (Knock et al., 2009). We here aimed to study the effect of delays on the FC structure and model performance in a neurophysiologically detailed model by recreating the irregular oscillations evident in MEG recordings in the alpha-band and relating the numerical simulations for different delays and the empirical data. For this, we employed a leaky-integrate-and-fire (LIF) spiking neuron model with realistic NMDA, AMPA and GABA synapses (Deco and Jirsa, 2012), and an oscillation-inducing calcium-dependent hyperpolarization current (triggering Spike-Frequency-Adaptation SFA; e.g. Fuhrmann et al., 2002; Liu and Wang, 2001; Meech, 1978). In the following, we will show that the presented model exhibits network oscillations in the alpha-range when the model nodes are coupled, and that it successfully captures alpha-band FC. It does so most robustly in the presence of delayed large scale connectivity, suggesting a functional importance for long-range delays in sustaining interaction patterns between areas and resting-state networks in the healthy brain.

Methods

Neuroanatomical connectivity matrix

Weighted neuroanatomical connectivity matrices were extracted from the diffusion tensor imaging (DTI) data of 21 healthy, normal participants (11 males, aged 22–45 years). Extraction methods were based on Gong et al. (2009). Diffusion MRI was acquired by using a single-shot echo planar imaging-based sequence with coverage of the whole brain; repetition time (TR), 9390 ms; echo time (TE), 65 ms. DTI images utilized 32 optimal nonlinear diffusion weighting directions ($b = 1200$ s/mm2) and 2 non-diffusion weighted volumes; reconstructed matrix = 128x128x45; reconstructed voxel size 2.0 mm × 2.0 mm × 2.0 mm. We also acquired T1-weighted structural images with a three-dimensional 'FLASH' sequence (TR = 12 ms, TE = 5.6 ms, flip angle = 19°, with elliptical sampling of k-space, giving a voxel size of 1 × 1 × 1 mm in 5.05 min). All scans were performed on the same Philips Achieva 1.5 Tesla Magnet. Weighted brain networks were constructed by first parcellating the brain, and then extracting the network from interregional connectivity analysis. Brain parcellation was constructed using the automated anatomical labeling (AAL, Tzourio-Mazoyer et al., 2002) template. The brain was parsed into 45 regions per hemisphere (90 in total), each region representing a node of the brain network. For each participant, parcellation was conducted in the diffusion MRI native space, and the b0 image was coregistered linearly to the T1-weighted structural image with the Flirt Tool (FMRIB, Oxford, Jenkinson et al., 2002). The transformed T1-weighted image was next mapped to the T1 template of ICBM152 in Montreal Neurological Institute (MNI) space (Collins et al., 1994), inversed, and further applied to warp the AAL mask from MNI space to the diffusion MRI native space, where interpolation using nearest-neighbor method ensured that the discrete labeling values were preserved. For the analysis of interregional connectivity (via Fdt toolbox in FSL, Oxford), diffusion MRI data was preprocessed by coregistering the diffusion-weighted images to a reference volume using an affine transformation for the correction of head motion as well as eddy current induced image distortion.

The local probability distribution of fiber direction and voxel connectivity probability were estimated via probabilistic tractography (Behrens et al., 2007), and the procedure was then extended to the level of each region. The connectivity probability from each of the parcellated brain regions to the other 89 regions was calculated. It must be noted that because of the dependence of tractography on the seeding location, the probability from i to j is not necessarily equivalent to that from j to i. However, these two probabilities are highly correlated across the brain for all subjects (the least Pearson $r = 0.70$, $p < 10^{-50}$). Therefore, the undirectional connectivity probability P_{ij} between region i and j was defined by averaging these two probabilities. Calculations of regional connectivity probability were implemented using in-house Perl scripts.

Finally, a weighted network graph was constructed by defining a distance and weight associated with each edge. The high connectivity probability between brain regions were taken here to be short distances

in a graph. Specifically, $W_{ij} = 1 - P_{ij}$ was computed as the distance/weight between brain region i and j, as used in previous literature (Achard and Bullmore, 2007). Note that the distance here does not correspond to the physical length of the white matter pathway linking the brain regions. For each subject, a 90 × 90 weighted cortical network/graph W was constructed, representing the anatomical organization of cerebral cortex.

MEG data collection and analysis

Data collection

MEG data were recorded from ten healthy participants who underwent a five minutes resting-state scan with their eyes closed. Recordings were performed at 1000 Hz sampling frequency on an Elekta Neuromag (Elekta Neuromag Oy, Helsinki, Finland) with 102 magnetometers and 102 pairs of orthogonal radial gradiometers. Subjects' head shape was recorded using a Polhemus Isotrack system, and four head position indicator (HPI) coils allowed for the head to be localized in the scanner.

Data analysis

Data preprocessing included signal space separation (Taulu et al., 2005), de-noising with independent component analysis, source reconstruction and bandpass filtering of the MEG signal. Signal space separation compensates for external interference and sensor artifacts by projecting the MEG data onto a basis set of spherical harmonics. Harmonics corresponding to sources originating from within the sensor array are preserved while interfering sources from outside the environment surrounding the sensor array are rejected. The sensor space MEG data were de-noised using temporal independent component analysis (ICA) to remove cardiac, 50 Hz mains and, in some subjects, eye movement artifacts.

Each dataset was then co-registered into the MNI space by registering the canonical MNI template to the Polhemus head shape data. A local sphere forward model (Huang et al., 1999) was then estimated using the subject's head shape. Both co-registration and forward model estimation were performed with the Matlab SPM8 package (FIL,UCL). The MEG data were then bandpass filtered into delta (1–5 Hz), theta (4–8 Hz), alpha (8–13 Hz), beta (13–30 Hz), low gamma (30–48Hz) and high gamma (52–80 Hz) bands. An LCMV beamformer was used to transform the original sensor time series for each frequency band into source space time series, that is, to reconstruct the activity at the 90 locations defined by the AAL brain parcellation.

Functional connectivity scores between node pairs were estimated by taking the band-limited power envelopes of a pair of nodes, regressing one out from the other to orthogonalize the time series and thereby removing any zero-lag correlations. We then calculated the Pearson correlation between the orthogonalized time series. Since the orthogonalization can be performed in both directions (X from Y and Y from X), the mean of both resulting correlation values was taken as the final correlation value. The full approach is described in detail and discussed in Brookes et al. (2012) and is the same as in Hipp et al. (2012). Functional connectivity scores between node pairs were estimated in the following way. For a given frequency band, a pair of nodes was selected. The first node of the pair was regressed from the second to orthogonalize the two time series, removing any zero-lag correlations induced by field spread. The correlation between the low pass filtered envelopes of the two orthogonalized time series was estimated.

This procedure was repeated but instead regressing the second voxel from the first and estimating the envelope correlation (Brookes et al., 2012; Hipp et al., 2012). The two different correlation values were then averaged to give a single correlation score. Here, we consider mainly the MEG signal's alpha BLP based on findings that, along with beta, it best captures the functional connectivity of RSN in MEG data (Brookes et al., 2011a, 2011b; Hipp et al., 2012; Luckhoo et al., 2012).

Global cortical model

The global model consists of 90 model nodes, each comprising an inhibitory and an excitatory pool of neurons, whose properties are described in detail below. Each node of the model represents one brain area, and the connections between any two nodes are implemented by interconnecting the respective neurons between the excitatory pools via NMDA and AMPA synapses. Transmission strengths are weighted by the corresponding value in the neuroanatomical connectivity matrix described above. As the DTI measure used to extract the structural connectivity is symmetrical, so are the connectivities in the model. Connections between nodes are limited to act between excitatory pools as they are here considered to represent long-range axons of pyramidal neurons. These connections are weighted by a global coupling factor W, which determines the overall connectivity strength in the resulting network. W, and the propagation velocity v are the main parameters to be varied in the simulations to find an area of parameter space where the correspondence between empirical and model data becomes maximal. In the brain, delays depend on axonal transmission times, which are determined by axon diameter, myelinization, and distance. The delay between two brain areas in the model was determined by their Euclidean distance in MNI-templated source space (max = 160 mm) divided by v, with propagation speed v in m/s and inter-area distance D in mm. The Euclidean distances are necessarily a lower bound estimate of fiber tract lengths, therefore propagation speeds would here be somewhat underestimated.

Local dynamics

Each node's local dynamics are modeled with 200 spiking neurons, featuring a biophysically realistic neural network model, consisting of leaky-integrate-and-fire (LIF) spiking neurons with NMDA, AMPA, and $GABA_A$ receptors (Brunel and Wang, 2001). The model was first adapted for modeling resting-state dynamics by, and is described in detail in Deco and Jirsa (2012). Their detailed global attractor model combines a realistic mechanistic model at the level of each single brain area with the large-scale cortical network structure. In the model, every node consists of an excitatory (index E, $N_E = 160$) and an inhibitory pool (index I, $N_I = 40$). The local dynamics are described by combining the dynamical equations of each neuron and the synaptic variables with all connected neurons. Excitatory/inhibitory neuron ratio and conductivities were balanced to reflect empirically realistic values and low spontaneous firing rates (DeFelipe, 1993; Destexhe et al., 1998) in each node (Fig. 3, inlay). Neurons inside a node were all-to-all connected in order to keep neuron numbers low and simulations feasible. There were N_E excitatory and N_I inhibitory presynaptic connections for every neuron, in addition to the excitatory inputs from long-range connections from pyramidal cells of other nodes and background input from 800 external neurons as described at the end of this paragraph. The neurons are modeled as LIF units that are characterized by the dynamics of their membrane potential. When the membrane voltage crosses a threshold V_{thr}, the neuron generates a spike, which is transmitted to connected neurons via its AMPA and NMDA or GABA synapses, and the membrane voltage is set to V_{reset}, where it is held fixed for the neuron's refractory period τ_{ref}. The subthreshold equation for the membrane potential is given by:

$$C_m^{E,I}\frac{dV(t)}{dt} = -g_m(V(t)-V_L) + I_{total}(t), \quad (1)$$

describing a basic RC-circuit with the cell membrane capacitance C_m in parallel with membrane resistance R_m, leak conductance $g_m = 1 / R_m$, resting potential $V_L = -70mV$, and synaptic and after-hyperpolarization (AHP) currents. Membrane time constants are given in Table 1. The total current I_{total} is the sum of synaptic external excitatory AMPA currents, AMPA and NMDA recurrent excitatory currents, GABAergic inhibitory currents and an after-hyperpolarization current

$$I_{total}(t) = I_{AMPA,ext}(t) + I_{AMPA}(t) + I_{NMDA}(t) + I_{GABA}(t) + I_{AHP}(t). \quad (2)$$

Table 1
Membrane and synaptic parameters.

Parameter	Excitatory ($N_E = 160$)	Inhibitory ($N_I = 40$)
C_m	0.5 nF	0.2 nF
g_m	25 nS	20 nS
V_L	−70 mV	70 mV
V_{thr}	−50 mV	50 mV
V_{reset}	−55 mV	55 mV
T_{ref}	2 ms	1 ms
gAM PA, ext	2.496 nS	1.944 nS
gAM PA, rec	0.104 nS	0.081 nS
gNM DA, rec	0.327 nS	0.258 nS
gGABA	4.375 nS	3.4055 nS

The synaptic currents and their mediation through gating variables $s_i^j(t)$ are described by:

$$I_{AMPA,ext}(t) = g_{AMPA,ext}(V(t)-V_E)\sum_{j=1}^{N_{ext}} s^j_{AMPA,ext}(t), \tag{3}$$

$$\frac{ds^j_{AMPA,ext}(t)}{dt} = \frac{s^j_{AMPA,ext}(t)}{\tau_{AMPA}} + \sum_k \delta\left(t-t_k^j\right), \tag{4}$$

$$I_{AMPA,rec}(t) = g_{AMPA,rec}(V(t)-V_E)\sum_{j=1}^{N_E} w_j s^j_{AMPA,ext}(t), \tag{5}$$

$$\frac{ds^j_{AMPA,rec}(t)}{dt} = \frac{s^j_{AMPA,rec}(t)}{\tau_{AMPA}} + \sum_k \delta\left(t-t_k^j\right), \tag{6}$$

$$I_{NMDA,rec}(t) = \frac{g_{NMDA,rec}(V(t)-V_E)}{1+\gamma e^{-\beta V(t)}}\sum_{j=1}^{N_E} w_j s^j_{NMDA,rec}(t), \tag{7}$$

$$\frac{ds^j_{NMDA,rec}(t)}{dt} = \frac{s^j_{NMDA,rec}(t)}{\tau_{NMDA,decay}} + \alpha x_j(t)\left(1-s^j_{NMDA,rec}(t)\right), \tag{8}$$

$$\frac{dx^j_{NMDA,rec}(t)}{dt} = \frac{x^j_{NMDA,rec}(t)}{\tau_{NMDA,rise}} + \sum_k \delta\left(t-t_k^j\right), \tag{9}$$

$$I_{GABA}(t) = g_{GABA}(V(t)-V_I)\sum_{j=1}^{N_I} w_j s^j_{GABA}(t), \tag{10}$$

$$\frac{ds^j_{GABA}(t)}{dt} = \frac{s^j_{GABA}(t)}{\tau_{GABA}} + \sum_k \delta\left(t-t_k^j\right), \tag{11}$$

with indices over neurons j, synaptic conductances g, excitatory and inhibitory reversal potentials V_E and V_I, respectively, the Dirac-delta function δ, and synaptic weight parameter w_j (determining the connection strengths between and within neural populations). NMDA currents are voltage dependent and modulated by intracellular calcium concentrations (Eq. (7)). Connections between excitatory and inhibitory pools were set to 1, and recurrent self-excitation to $w_+ = 1.5$. Synaptic parameters were $V_E = 0$ mV, V_I = -70 mV, $\tau_{AMPA} = 2$ ms, $\tau_{NMDA,rise} = 2$ ms, $\tau_{NMDA,decay} = 100$ ms, $\tau_{GABA} = 10$ ms, $\alpha = 0.5$ kHz, $\beta = 0.062$, and $\gamma = 0.28$. The remaining constant neural parameters are given in Table 1.

The adaptation-inducing calcium-dependent AHP current I_{AHP} is given by:

$$I_{AHP}(t) = -g_{AHP}Ca(t)(V(t)-V_K), \tag{12}$$

$$\frac{dCa(t)}{dt} = -\frac{Ca(t)}{\tau_{Ca}} + \alpha_{CA}\sum_i \delta(t-t_i), \tag{13}$$

where $\alpha_{Ca} = .2$, $\tau_{Ca} = 70$ ms, $g_{AHP} = 100$ nS, and were chosen to induce alpha-range oscillations in the presence of network input. For a more detailed discussion on the dependency of adaptation-induced oscillations on the input and the time constant, see Augustin et al. (2013). Note that we here focused on the implementation of noisy oscillations as opposed to fixed frequency oscillators or to the asynchronous state, and manually adjusted the SFA values to introduce heterogeneous alpha-activity into the model. Parameters were based on previously established values (Brunel and Wang, 2001; Ermentrout et al., 2001) guided by physiological measurements (Ahmed et al., 1998; Helmchen et al., 1996; Svoboda et al., 1997).

All neurons in the network received an external background input from $N_{ext} = 800$ external AMPA signaling excitatory neurons injecting uncorrelated Poisson-distributed spike trains, representing the noisy fluctuations that are typically observed in vivo. Specifically, for all neurons inside a given population p, the rate v^p_{ext} of the resulting global spike train is described by:

$$\tau_n \frac{dv^p_{ext}(t)}{dt} = -\left(v^p_{ext}(t)-v_0\right) + \sigma_v \sqrt[2]{2\tau_n}\, n^p(t) \tag{14}$$

where $t_n = 300$ ms, $v_0 = 2.4$ kHz, σ_v is the standard deviation of $v^p_{ext}(t)$, and $n^p(t)$ is normalized Gaussian white noise. Negative values of $v^p_{ext}(t)$ that could arise due to the noise term are rectified to zero. The resulting simulated time series was calculated by summing up all synaptic input currents (AMPA, GABA and NMDA). This signal more directly corresponds to a simulated LFP signal (as in e.g. Mazzoni et al., 2008) than to the dendritic currents the MEG signal originates in, but some evidence from simultaneous intracortical recordings and MEG during tactile stimulation suggests good correspondence between LFP and MEG signals (Zhu et al., 2009). This may be due to the fact that though dendritic integration of synaptic input may be highly nonlinear due to dendrite shape, this effect may be balanced by ion channel distribution and synaptic properties, which can cancel dendritic signal distortion (Magee, 2000). Power envelopes were calculated analogously to those of MEG recordings.

Results

We present a theoretical model of spontaneous brain activity that specifically considers the noisy oscillatory nature evident in MEG resting-state recordings. The model is based on local LIF-neuronal dynamics of populations of inhibitory and excitatory neurons, combined with a structural connectivity matrix that determines inter-areal connection strengths. Oscillations emerge in the model from the recurrent input between nodes, paired with neural adaptation in each node. Considering the noisy oscillations of the empirical data and the model, we show in the following that the model captures the network connectivity of the MEG resting-state data in an optimal limited range of global coupling strengths. The inclusion of neurophysiologically realistic delays shifts the working point to higher mean coupling values and increases the concordance between model and empirical data.

MEG data

In the literature, resting-state activity has been associated primarily with BLP in the alpha- and beta-bands (Brookes et al., 2011a, 2011b; Mantini et al., 2007). In line with these findings, the power spectrum of the MEG data set from the present study had a peak around 10 (8–12) Hz (Fig. 2, first panel). Though typically the characteristics (e.g. peak location, frequency differences between areas, peak amplitude) vary across persons, age and sex groups, its appearance is a very robust finding (Chiang et al., 2011). In our group of 10 healthy adult subjects, the mean power spectral peak was centered at 8.7 Hz ($\pm$2.25). The data was low-passed filtered and freed from artifacts as described in detail in the methods section. When filtering the time series in 15 bands of

4 Hz width from 0 to 60 Hz, the alpha-band also carries the highest mean BLP connectivity between nodes.

Brookes et al. (2011b) showed resting-state networks resembling those previously found in fMRI studies for these MEG recordings. Using ICA, they independently identified eight RSN in the MEG alpha- and beta-band power envelopes closely coinciding with RSN also found in fMRI recordings (their Fig. 1: a) DMN in alpha; b) left lateral frontoparietal, c) right lateral frontoparietal, d) sensorimotor, e) medial parietal, f) visual, g) frontal and anterior cingulate, and h) cerebellar networks). Focusing here on the oscillatory data component and studying the effect of long-range delays on the model FC structure over a range of coupling and delay parameters, we directly fitted the model FC to the empirical alpha power FC structure. Graph measures for the empirical FC matrix are shown in Supplementary Fig. 1.

Model data

The model consisted of local nodes connected to each other by long-range connections. The structure of these long-range connections was fixed as it was based on neuroanatomical DTI measurements. Additionally, two free parameters shaped the spatiotemporal network structure. Connectivity strength between nodes was varied systematically with coupling parameter W, and the spatiotemporal pattern of the connectivity was modulated by introducing global propagation velocity parameter v, which changed the temporal dynamics of the network. W is unitless and unknown and was the main free parameter in the model, and we varied v from Infinity (no delays) across a physiological range of delays (5.10 m/s) to very large delays (1 m/s).

In the model, isolated nodes did not oscillate autonomously or from the background activity only. Increasing input from other nodes triggered activity-dependent SFA, leading itself to noisy oscillations in the alpha-band (Fig. 2). The shape of the model frequency spectrum thus depended on the global coupling parameter W: increasing the coupling between brain areas caused the network nodes to start oscillating at around 10 Hz, at a similar frequency as the alpha-peak evident in the MEG data. When coupling was further increased, the network oscillations became more and more regular. The transition from the low asynchronous state over noisy oscillations with irregular spiking across all pools of neurons to the highly regular population spikes for high W can be seen for one brain area example time series in Fig. 3. Oscillatory power and peak frequency further depended on the mean input (Fig. 2, bottom panels).

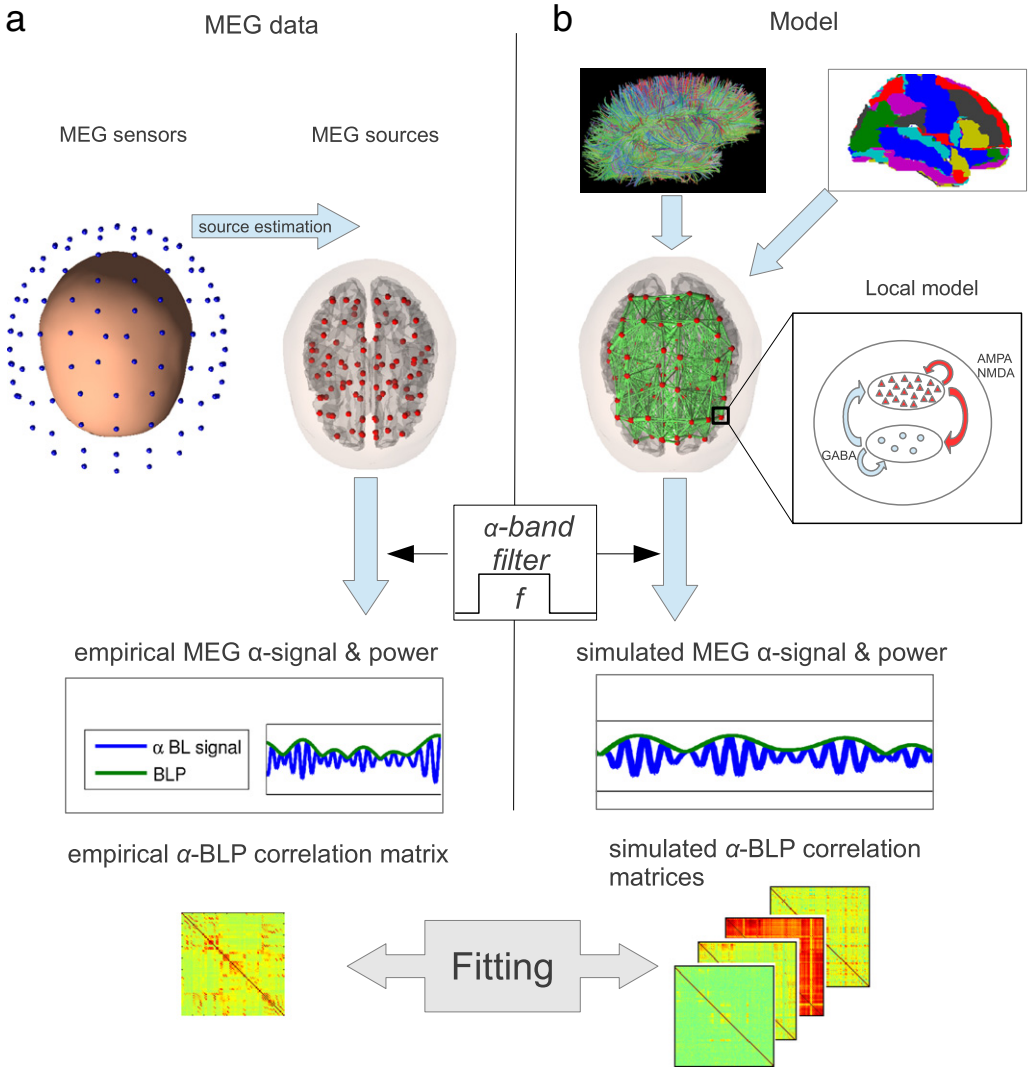

Fig. 1. Data processing and analysis: a) MEG time series are recorded by sensors and transformed into AAL source-space time series with a beamformer algorithm. The resulting time series for each brain area was then filtered in the alpha-band (8–12 Hz) and its BLP was extracted via Hilbert-envelope computation, resulting in 90 alpha-power time series. b) The model was constructed by taking the same AAL brain parcellation used for source-reconstruction of the MEG signal, and putting a model node in the center of each brain area. LIF neuron populations determined the local node dynamics, and DTI-measurements determined the connection weights between nodes (see Methods section). The connected network was simulated for 5 min, and the resulting simulated LFP's band-pass filtered alpha-power envelopes were calculated the same way as for MEG recordings.

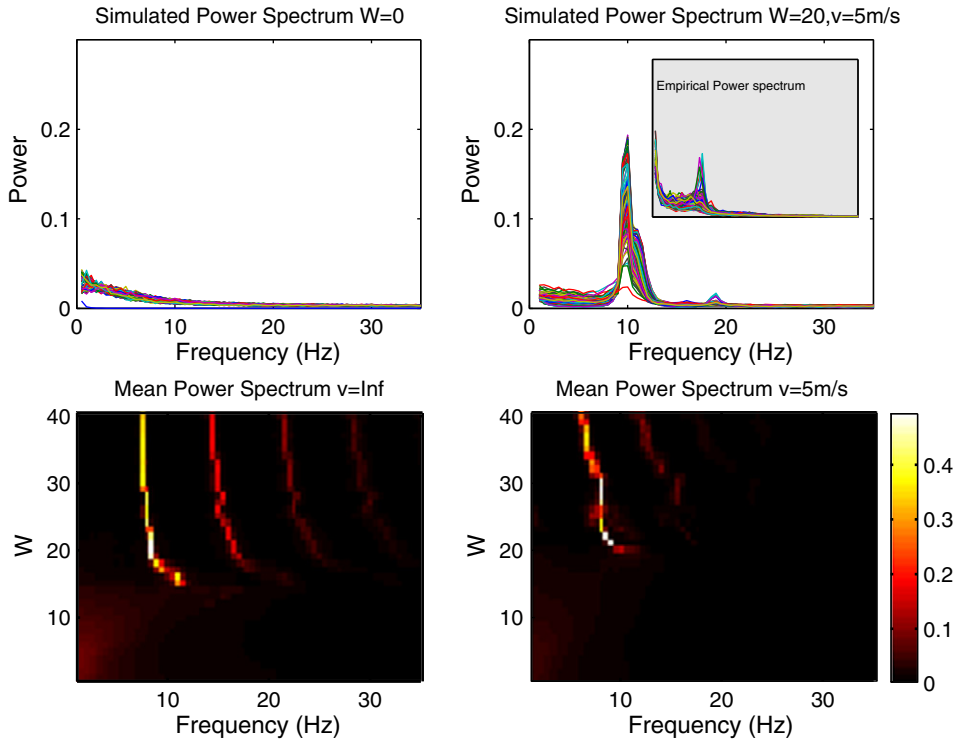

Fig. 2. Top: power spectra for all brain areas/nodes for exemplary simulation with disconnected nodes ($W = 0$, top left) and at $W = 20, v = 5$ m/s (top right). The inlay shows the mean power spectrum for empirical MEG recordings. Bottom: mean power spectra over all nodes for undelayed (left) and delayed (right) simulations.

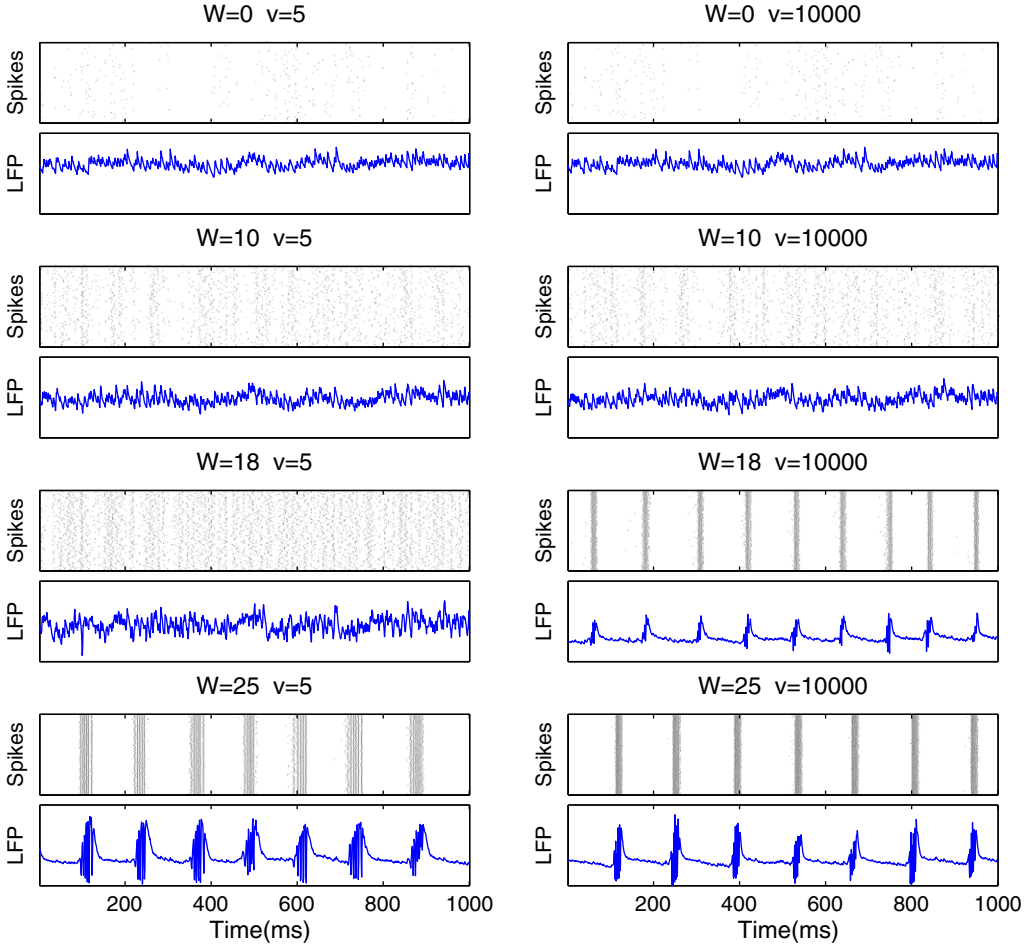

Fig. 3. Example raw time series for one brain area (PCC) over one second for different cortical processing speed v (left column: 5 m/s, right column: No delays) and different global coupling values W.

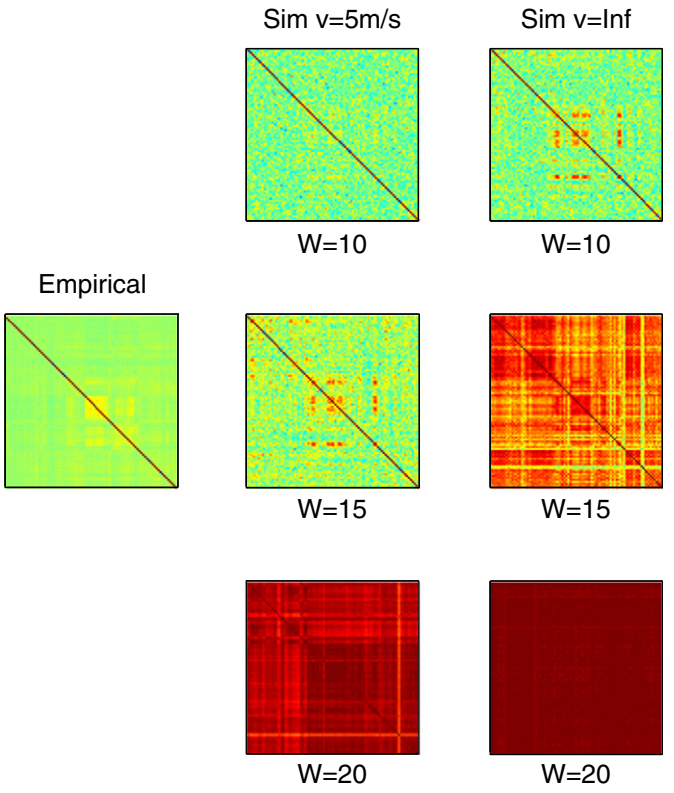

Fig. 4. FC matrices for empirical (first column) and simulated data at different delays and couplings (second and third column). High synchrony appears much earlier in the absence of delays (third column) as oscillations become more regular (see Fig. 3).

Model fit

For each simulation in parameter space of W and v, we extracted the BL alpha-power and calculated the FC from each node to each other node (Fig. 4). To judge the model's performance and find the optimal working point, we systematically varied W and v, and compared the resulting model FC matrices between model nodes with the corresponding MEG derived FC. After applying a Fisher-Z transform to the FC measures (due to the non-additivity of correlation coefficients, Zimmerman et al., 2003), the matrices unique triangular parts were vectorized and the performance of the model was then calculated from the Pearson correlation between MEG data and model.

Fig. 5 shows the model performance defined by alpha range power envelope correlations for a range of W and v parameters. The ability of the model to capture the empirical functional connectivity depends on the coupling strength and propagation speed. For weak couplings, there is no connection between the model nodes, and all nodes have independent activity. For intermediate couplings, the network nodes couple dynamically and trigger the SFA. A performance peak of the model in predicting the empirical FC in the alpha-BLP can be found with this intermediate coupling range for all delay levels, the maximal fit being reached at lower coupling levels for smaller delays, and the performance curve flattening out for very large delays (1 m/s) (remaining low for higher couplings, not shown). Also note that delays increase the region of global coupling values for which the model yields a good prediction of the empirical FC: the range of global coupling values for which the fit is systematically rising beyond .10 (orange/yellow in Fig. 5, bottom) is much wider for intermediate delays at 5 m/s than for v = Inf. See Supplementary Fig. 2 for model performance and correlation distances for frequency bands from delta to high gamma-bands, which shows highest maximal fits for the alpha range, decreasing both towards lower and higher frequency bands.

Fig. 6 shows the FC pattern of two brain areas pertaining to distinct networks: the left posterior cingulate (DMN) and left dorsomedial frontal cortex (associated with task control). The functional differences of the regions are reflected by their embedding in different networks at rest, and functional connections between nodes without direct structural links can be observed both in the MEG data and in the model.

The here presented model is quite different from simpler oscillator models such as presented by Cabral et al. (2011) and Deco et al. (2009) where delays play a critical role in maintaining phase heterogeneity between the nodes. In the spiking model, complete synchronization is prevented for most of parameter space by the heterogeneity and size of the network, through background noise and a wider distribution in time of individual spike times. Therefore, delays are not

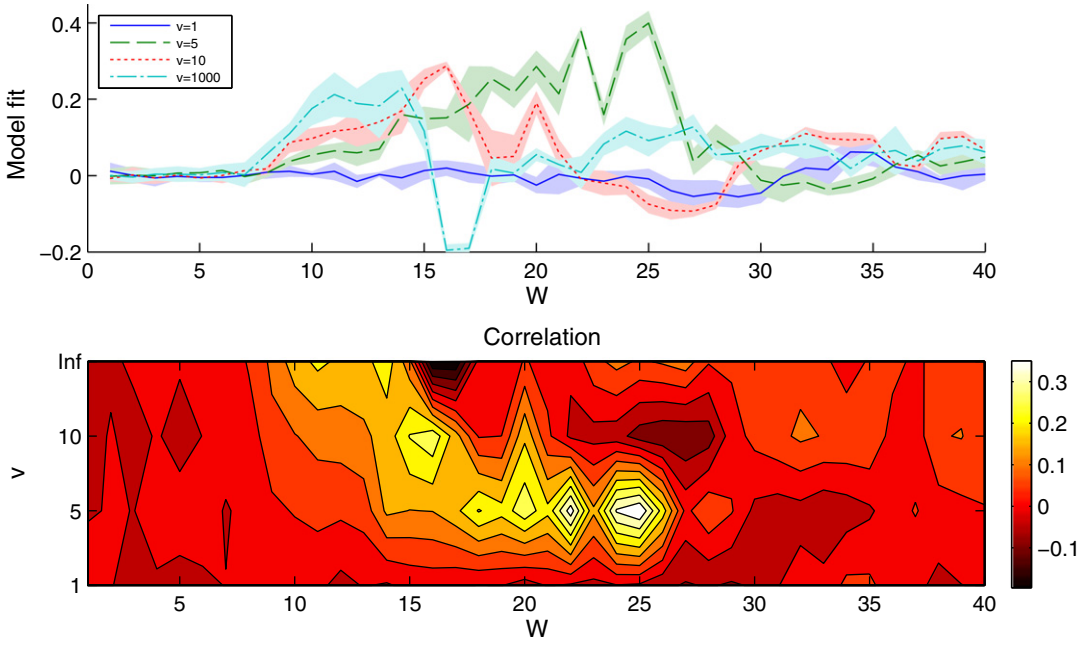

Fig. 5. Empirical fit: model performance as measured by Pearson correlation between empirical and model FC, based on alpha band-limited power correlations, with Error bars (standard deviation over 5 trials, top), and a color representation for mean over trials (bottom). Maximal fit of r = .40 is reached at W = 25, v = 5.

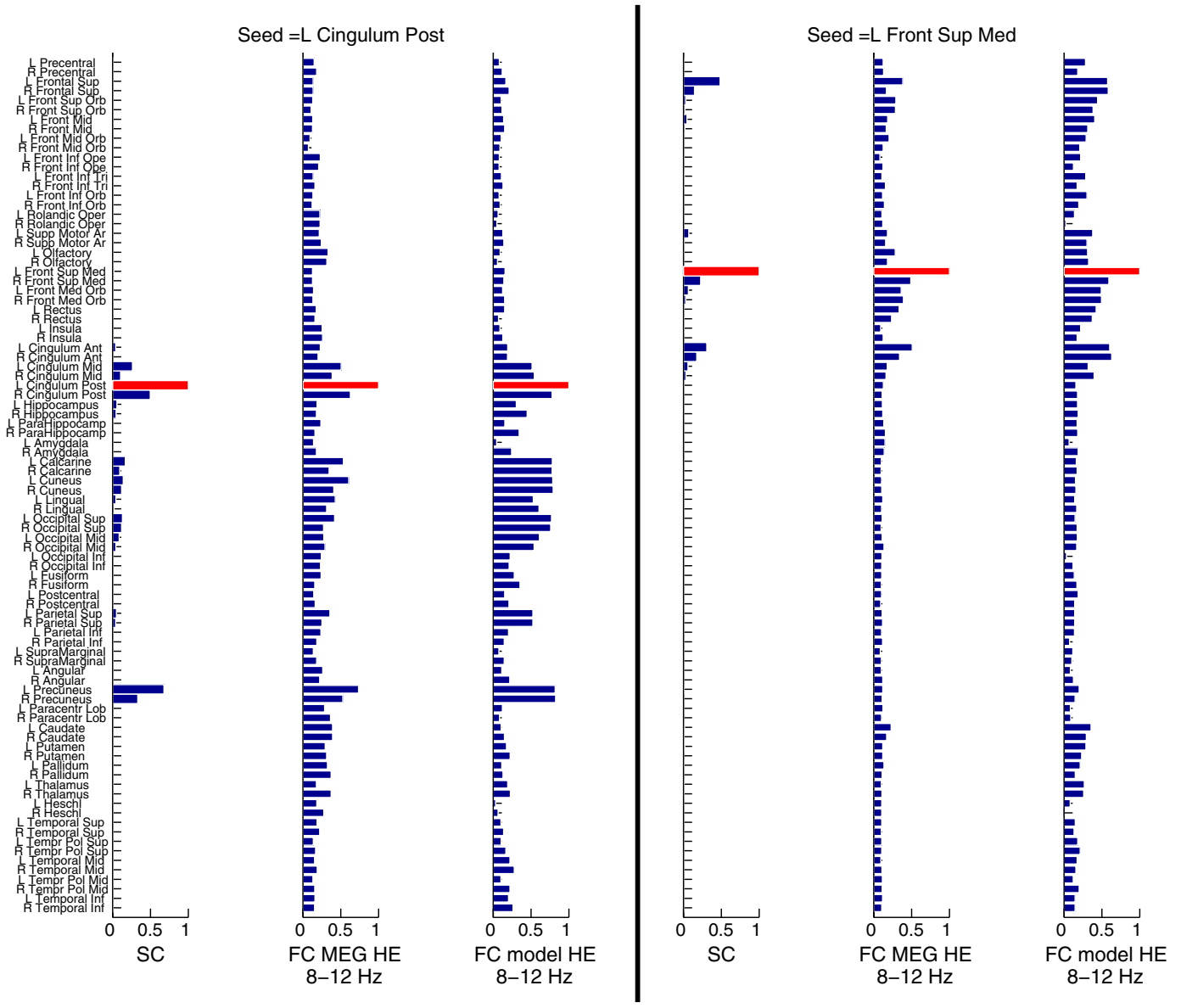

Fig. 6. SC, empirical FC and model FC of the alpha-band power envelopes (HE) for left posterior Cingulate Cortex (left) and left dorsomedial Frontal Cortex (right).

critically necessary for a good model fit. They do, however, change the spatiotemporal connectivity pattern. As a result, strong connection inputs are more evenly distributed in time and mean firing rate is reduced, and with it SFA. Without delays, all inputs into a pool arrive at the same time, and therefore sum up to higher momentary inputs. With delays, time differences between the arrival of inputs from other brain areas are introduced. In theory, in spontaneous activity, this change in temporal connectivity may also lead to synchronizing strong inputs in some cases. Effectively, though, the introduction of delays distributes inputs from different nodes in time. This leads on the one hand to higher required global coupling to effectuate changes in node activity in a nonlinear system where single weak activities may drown in the background noise. On the other hand, due to delays, there is also a less abrupt accumulation of the AHP-current and a later transition to regular oscillations for the delayed case (Fig. 3, center row, left vs right column: while for $v = 5$, spiking is still quite irregular, the same global coupling without delays already shows population bursts). For even higher couplings, the system transitions to a high firing regular oscillation regime for all delays, as visible both in the spike raster plots and the LFP time series in Fig. 3.

Discussion

In this study, we investigated how spontaneous brain activity, oscillations and functional connectivity as recorded by MEG may be captured in a neurophysiological resting-state model. To this aim, we equipped a local LIF-neuron population model (Deco and Jirsa, 2012) with SFA and implemented it on the nodes of a neuroanatomically based large-scale brain connectivity graph. Our results demonstrate that the model captures the network connectivity patterns in band-limited alpha-power, and that it does so most robustly in the presence of cortical transmission delays.

Spatial patterns of fMRI resting-state activity have been reproduced in the last years with a variety of models (Cabral et al., 2011; Deco and Jirsa, 2012; Deco et al., 2009; Ghosh et al., 2008a,b; Honey et al., 2007, 2009). In these models, network dynamics in resting-state models are importantly shaped by three key factors: couplings, delays and noise (Deco et al., 2009). In all the models, the coupling matrix between the nodes plays a crucial role in shaping the spatial patterns of activity. The role of delays and noise, however, depend more on the specific local dynamics used to model neural activity. For example, neither delays nor

external noise are necessary to keep the system dynamic and activated in the case of chaotic dynamics (Honey et al., 2007, 2009). In other cases, noise is essential to introduce transitions between multistable states (Deco and Jirsa, 2012; Deco et al., 2009; Ghosh et al., 2008a, 2008b). Noise can be neglected also in a complex network arrangement of Kuramoto oscillators with delays, which may show ongoing dynamics and transient couplings (so called Chimera states) (Cabral et al., 2011). Delays, in general, do not influence slow asynchronous dynamics (Deco and Jirsa, 2012), but become essential in the case of underlying oscillatory dynamics on the time scale of the delays (Jirsa, 2009; Jirsa and Ding, 2004). When assuming intrinsic nonchaotic oscillatory dynamics in the local nodes (Cabral et al., 2011; Deco et al., 2009; Ghosh et al., 2008a,b), delays are necessary to prevent full synchronization of the network. In a FitzHugh–Nagumo oscillator model, Knock et al. (2009) showed that characteristics of the connectivity matrix matter for the importance of delays in shaping dynamics and found that the network structure is less affected by delay magnitude changes for symmetric than for asymmetric graphs. This is due to real symmetric matrices having real eigenvalues, so the networks equilibrium point may change with connectivity, but not the dynamics (though note that DSI matrices may also show asymmetries due to normalization of connectivity by brain area size, resulting in larger weights from larger areas to smaller ones than vice-versa). This may, however, depend on the specific model, as e.g. in the model of Cabral et al. (2011), delays shape the spatiotemporal structure of the oscillators, whose phase interactions, and therefore clustering and frequency suppression, depend on the spatiotemporal layout in a DSI-derived SC network. In the here presented model, delays are important to consider as they shape network dynamics and increase the model fit in a physiological delay range.

We focused on alpha-band activity due to alpha being the most distinguished oscillatory rhythm during eyes-closed resting-state, and to exemplarily address the question of how the spatiotemporal connectivity structure and presence of physiological, noisy oscillations interact to form network dynamics. Due to these dynamics occurring mainly in the alpha-range, this is also where the highest fits were found, followed by the beta- and theta-bands (Supplementary Fig. 2). The advantage of this model is the spontaneous emergence of noisy oscillations in the network. Oscillations are important to consider when investigating RSN and resting-state FC in the light of its neuronal dynamics and mechanisms, as we have seen from recent EEG/fMRI and MEG studies. Though the functions and details of origins of these oscillations are still undetermined, we can study their dynamics and properties with oscillatory models, where the critical settings and oscillatory dynamics depend on the specific model applied. In the Kuramoto model, for example, oscillations emerge due to the tendency of coupled oscillators to synchronize, leading to clusters of nodes transiently synchronizing at reduced frequencies, and are based on the intrinsically (gamma-band) oscillatory nature of the nodes.

The here employed SFA mechanism parsimoniously creates alpha-oscillations based on an easily physiologically interpretable biological mechanism. Noisy oscillations emerge for the intermediate parameter range where the model best fits the data also in terms of functional connectivity, and naturally reproduces some details of empirically observable alpha-rhythms, such as the higher amplitude and frequency peaks for occipital nodes. This may be due to higher adaptation in visual areas, but also arises naturally in the model, as the oscillation frequency depends on the interplay of neural adaptation and recurrent excitatory input, and occipital nodes are more interconnected on average. As an outlook, the reduction of alpha-rhythms typically seen during tasks could be easily modulated by arousal-related ACh signaling (which reduces adaptation). We here focus on simulating the network in a full spiking model to consider the heterogeneous spike times, and their stabilizing effect on the system's oscillatory response, as well as to allow for a direct physiological interpretation of the oscillatory source. This, however, makes it difficult to explore the stability of the network behavior over a large parameter space, and reduced models are needed to investigate regime bifurcations and to study parameter interactions in more detail. These relations (Deco et al., 2013a, 2013b; Jirsa, 2009) and the origins and dynamics of alpha activities (e.g. Augustin et al., 2013; Freyer et al., 2011, 2012) are under active investigation, and will help us in the future to further specify the oscillatory sources of models and study their impacts and influences on the network dynamics.

We here implemented SFA as an oscillation-generating mechanism in order to study the importance of delays in the presence of noisy network oscillations. The detailed origins, dynamics, and modulation of spontaneous oscillatory activity and causal role of adaptation in the brain in its different states, however, need to be studied in much more depth. In the brain, various types of adaptation currents in cortical neurons exist, differing in strength between layers. They are modulated by various factors such as polarization state (Connors et al., 1982; Llinas, 1988), cortical depth (Ahmed et al., 1998), and cholinergic signaling (Crook et al., 1998). These interdependencies and more systematic variation of adaptation parameters in (reduced) large-scale cortical models may be of great help to understand spontaneous brain dynamics and states in the future.

Though beyond the scope of this study, it is noteworthy that the bursting mode observed here for sufficiently strong adaptation and recurrency (Fig. 3), while not resembling the oscillatory dynamics of the resting-state, are much more reminiscent of up and down states in sleep dynamics (e.g. Steriade, 1997), though at different frequencies. The relation between acetylcholine signaling and cortical activation and cognitive states on one hand (Sarter and Bruno, 1999; Vazquez and Baghdoyan, 2001) and SFA on the other hand (Stiefel et al., 2009) may help us in the future to better understand spontaneous brain dynamics in wake and sleep. This transition was studied in a layered model of thalamus and portions of visual cortical areas by Hill and Tononi (2005), and by Deco et al. (2013a) in a cortical model for slow waves. A key challenge for future work will be to consider these modulations, and to study the key responsible mechanisms, resulting network dynamics and interactions in whole-brain models for different frequency bands.

In the presented data, maximal model fit was no higher than .4 for any delay condition, which leaves room for improvement. Of course, this may be related to dynamics and communications not captured by the model, such as, e.g., lateral connections (Spiegler and Jirsa, 2013), or directionality of fibers between brain areas. Results are also influenced by the quality of the DTI matrix, which is prone to miss interhemispheric connections (Hagmann et al., 2008). There is ongoing work in our lab to enhance the quality of the DTI by integrating FC and SC through a modeling approach. The DTI acquisition parameters from the used dataset at 1.5 T and $b = 1200$ may also have limited the SC precision. Another aspect to consider is the choice of brain parcellation and preprocessing, which may influence connectivity estimates (Cloutman and Lambon Ralph, 2012; Van Essen et al., 2012; Wang et al., 2009; Zalesky et al., 2010). Here, an AAL parcellation without volume normalization for the DTI was used. From a model and connectivity perspective, smaller brain areas are favorable, although MEG signal leakage limits the spatial resolution. Importantly, though these issues need to be studied in more detail, they should not be critical in the main findings of the current study, as we focus on the relative changes and effects of including delays rather than the exact network structure.

In conclusion, brain connectivity and resting-state FC investigation is becoming more and more important, both for understanding basic organization principles of brain networks as well as for investigating and potentially diagnosing medical conditions. With access to neurophysiological recordings of resting-state activity at high temporal resolutions, we are now in the position to investigate the importance of oscillation in the brain for spontaneous network patterns. We here propose a model that offers an implementation of such noisy oscillations combined with large-scale resting-state network connectivity. We demonstrate that in the presence of these oscillatory dynamics, the model

best captures the band-limited power connectivity patterns of the empirical data when considering delays.

Supplementary data to this article can be found online at http://dx.doi.org/10.1016/j.neuroimage.2013.11.009.

Acknowledgments

TTN was supported by the SUR of the DEC of the Catalan Government and by the FSE. GD was supported by the ERC Advanced Grant: DYSTRUCTURE (n. 295129), by the Spanish Research Project SAF2010-16085 and by the CONSOLIDER-INGENIO 2010 Programme CSD2007-00012, and the FP7-ICT BrainScales. The research reported herein was supported by the Brain Network Recovery Group through the James S. McDonnell Foundation. MJ was supported by the MINDLab Investment Capital for University Research Fund. MLK was supported by the TrygFonden Charitable Foundation. We thank Sven L. Hilbert and Katharina Glomb for useful discussions on earlier versions of this manuscript and two anonymous reviewers for their helpful comments and suggestions.

Conflict of interest

The authors declare to have no conflicts of interest.

References

Achard, S., Bullmore, E., 2007. Efficiency and cost of economical brain functional networks. PLoS Comput. Biol. 3, e17. http://dx.doi.org/10.1371/journal.pcbi.0030017.

Ahmed, B., Anderson, J.C., Douglas, R.J., Martin, K.A., Whitteridge, D., 1998. Estimates of the net excitatory currents evoked by visual stimulation of identified neurons in cat visual cortex. Cereb. Cortex 8, 462–476. http://dx.doi.org/10.1093/cercor/8.5.462 (URL: http://cercor.oxfordjournals.org/content/8/5/462.abstract).

Augustin, M., Ladenbauer, J., Obermayer, K., 2013. How adaptation shapes spike rate oscillations in recurrent neuronal networks. Front. Comput. Neurosci. 7, 9. http://dx.doi.org/10.3389/fncom.2013.00009 (URL: http://www.frontiersin.org/Computational_Neuroscience/10.3389/fncom.2013.00009/abstract).

Behrens, T., Berg, H.J., Jbabdi, S., Rushworth, M., Woolrich, M., 2007. Probabilistic diffusion tractography with multiple fibre orientations: What can we gain? NeuroImage 34, 144–155. http://dx.doi.org/10.1016/j.neuroimage.2006.09.018 (URL: http://www.sciencedirect.com/science/article/pii/S1053811906009360, cited by 0787).

Ben-Simon, E., Podlipsky, I., Arieli, A., Zhdanov, A., Hendler, T., 2008. Never resting brain: simultaneous representation of two alpha related processes in humans. PLoS ONE 3, e3984. http://dx.doi.org/10.1371/journal.pone.0003984 (URL: http://www.ncbi.nlm.nih.gov/pubmed/19096714. PMID: 19096714).

Biswal, B., Yetkin, F.Z., Haughton, V.M., Hyde, J.S., 1995. Functional connectivity in the motor cortex of resting human brain using echo-planar MRI. Magn. Reson. Med. 34, 537–541 (URL: http://www.ncbi.nlm.nih.gov/pubmed/8524021. PMID: 8524021).

Biswal, B.B., Kylen, J.V., Hyde, J.S., 1997. Simultaneous assessment of flow and BOLD signals in resting-state functional connectivity maps. NMR Biomed. 10, 165–170. http://dx.doi.org/10.1002/(SICI)1099-1492(199706/08)10:4/5<165::AID-NBM454>3.0.CO;2-7 (URL: http://onlinelibrary.wiley.com/doi/10.1002/(SICI)1099-1492(199706/08)10:4/5%3C165::AID-NBM454%3E3.0.CO;2-7/abstract).

Brookes, M.J., Hale, J.R., Zumer, J.M., Stevenson, C.M., Francis, S.T., Barnes, G.R., Owen, J.P., Morris, P.G., Nagarajan, S.S., 2011a. Measuring functional connectivity using MEG: methodology and comparison with fcMRI. NeuroImage 56, 1082–1104. http://dx.doi.org/10.1016/j.neuroimage.2011.02.054 (URL: http://www.sciencedirect.com/science/article/pii/S1053811911002102).

Brookes, M.J., Woolrich, M., Luckhoo, H., Price, D., Hale, J.R., Stephenson, M.C., Barnes, G.R., Smith, S.M., Morris, P.G., 2011b. Investigating the electrophysiological basis of resting state networks using magnetoencephalography. Proc. Natl. Acad. Sci. U. S. A. http://dx.doi.org/10.1073/pnas.1112685108 (URL: http://www.pnas.org/content/early/2011/09/14/1112685108.abstract).

Brookes, M.J., Woolrich, M.W., Barnes, G.R., 2012. Measuring functional connectivity in MEG: a multivariate approach insensitive to linear source leakage. NeuroImage 63, 910–920. http://dx.doi.org/10.1016/j.neuroimage.2012.03.048 (PMID: 22484306).

Brunel, N., Wang, X.J., 2001. Effects of neuromodulation in a cortical network model of object working memory dominated by recurrent inhibition. J. Comput. Neurosci. 11, 63–85.

Buckner, R.L., Andrews-Hanna, J.R., Schacter, D.L., 2008. The brain's default network. Ann. N. Y. Acad. Sci. 1124, 1–38. http://dx.doi.org/10.1196/annals.1440.011 (URL: http://onlinelibrary.wiley.com/doi/10.1196/annals.1440.011/abstract).

Cabral, J., Hugues, E., Sporns, O., Deco, G., 2011. Role of local network oscillations in resting-state functional connectivity. NeuroImage. http://dx.doi.org/10.1016/j.neuroimage.2011.04.010 (URL: http://www.ncbi.nlm.nih.gov/pubmed/21511044. PMID: 21511044).

Chiang, A.K.I., Rennie, C.J., Robinson, P.A., Van Albada, S.J., Kerr, C.C., 2011. Age trends and sex differences of alpha rhythms including split alpha peaks. Clin. Neurophysiol. 122, 1505–1517.

Cloutman, L.L., Lambon Ralph, M.A., 2012. Connectivity-based structural and functional parcellation of the human cortex using di_usion imaging and tractography. Front. Neuroanat. 6, 34. http://dx.doi.org/10.3389/fnana.2012.00034 (PMID: 22952459).

Collins, D.L., Neelin, P., Peters, T.M., Evans, A.C., 1994. Automatic 3D intersubject registration of MR volumetric data in standardized talairach space. J. Comput. Assist. Tomogr. 18, 192–205 (PMID: 8126267).

Connors, B.W., Gutnick, M.J., Prince, D.A., 1982. Electrophysiological properties of neocortical neurons in vitro. J. Neurophysiol. 48, 1302–1320 (URL: http://jn.physiology.org/content/48/6/1302).

Cordes, D., Haughton, V.M., Arfanakis, K., Wendt, G.J., Turski, P.A., Moritz, C.H., Quigley, M.A., Meyerand, M.E., 2000. Mapping functionally related regions of brain with functional connectivity MR imaging. AJNR Am. J. Neuroradiol. 21, 1636–1644 (URL: http://www.ajnr.org/content/21/9/1636).

Cordes, D., Haughton, V.M., Arfanakis, K., Carew, J.D., Turski, P.A., Moritz, C.H., Quigley, M.A., Meyerand, M.E., 2001. Frequencies contributing to functional connectivity in the cerebral cortex in "Resting-State" data. AJNR Am. J. Neuroradiol. 22, 1326–1333 (URL: http://www.ajnr.org/content/22/7/1326).

Cordes, D., Haughton, V., Carew, J.D., Arfanakis, K., Maravilla, K., 2002. Hierarchical clustering to measure connectivity in fMRI resting-state data. Magn. Reson. Imaging 20, 305–317. http://dx.doi.org/10.1016/S0730-725X(02)00503-9 (URL: http://www.sciencedirect.com/science/article/pii/S0730725X02005039).

Crook, S.M., Ermentrout, G.B., Bower, J.M., 1998. Spike frequency adaptation affects the synchronization properties of networks of cortical oscillators. Neural Comput. 10, 837–854. http://dx.doi.org/10.1162/089976698300017511.

Damoiseaux, J.S., Rombouts, S.A.R.B., Barkhof, F., Scheltens, P., Stam, C.J., Smith, S.M., Beckmann, C.F., 2006. Consistent resting-state networks across healthy subjects. Proc. Natl. Acad. Sci. U. S. A. 103, 13848–13853. http://dx.doi.org/10.1073/pnas.0601417103 (URL: http://www.pnas.org/content/103/37/13848.abstract).

De Luca, M., Smith, S., De Stefano, N., Federico, A., Matthews, P.M., 2005. Blood oxygenation level dependent contrast resting state networks are relevant to functional activity in the neocortical sensorimotor system. Exp. Brain Res. 167, 587–594. http://dx.doi.org/10.1007/s00221-005-0059-1 (PMID: 16284751).

De Luca, M., Beckmann, C.F., De Stefano, N., Matthews, P., Smith, S., 2006. fMRI resting state networks de_ne distinct modes of long distance interactions in the human brain. NeuroImage 29, 1359–1367. http://dx.doi.org/10.1016/j.neuroimage.2005.08.035 (URL: http://www.sciencedirect.com/science/article/pii/S1053811905006257).

de Pasquale, F., Della Penna, S., Snyder, A.Z., Lewis, C., Mantini, D., Marzetti, L., Belardinelli, P., Ciancetta, L., Pizzella, V., Romani, G.L., Corbetta, M., 2010. Temporal dynamics of spontaneous MEG activity in brain networks. Proc. Natl. Acad. Sci. U. S. A. 107, 6040–6045. http://dx.doi.org/10.1073/pnas.0913863107 (URL: http://www.pnas.org/content/107/13/6040.abstract).

Deco, G., Corbetta, M., 2011. The dynamical balance of the brain at rest. Neuroscientist 17, 107–123. http://dx.doi.org/10.1177/1073858409354384 (URL: http://nro.sagepub.com/content/17/1/107.abstract).

Deco, G., Jirsa, V.K., 2012. Ongoing cortical activity at rest: criticality, multistability, and ghost attractors. J. Neurosci. 32, 3366–3375. http://dx.doi.org/10.1523/JNEUROSCI.2523-11.2012 (URL: http://www.jneurosci.org/content/32/10/3366,).

Deco, G., Jirsa, V.K., McIntosh, A.R., Sporns, O., Kotter, R., 2009. Key role of coupling, delay, and noise in resting brain fluctuations. Proc. Natl. Acad. Sci. U. S. A. 106, 10302.

Deco, G., Jirsa, V.K., McIntosh, A.R., 2013a. Resting brains never rest: computational insights into potential cognitive architectures. Trends Neurosci. 36, 268–274. http://dx.doi.org/10.1016/j.tins.2013.03.001 (URL: http://www.sciencedirect.com/science/article/pii/S0166223613000398, cited by 0001).

Deco, G., Ponce-Alvarez, A., Mantini, D., Romani, G.L., Hagmann, P., Corbetta, M., 2013b. Resting-state functional connectivity emerges from structurally and dynamically shaped slow linear fluctuations. J. Neurosci. 33, 11239–11252. http://dx.doi.org/10.1523/JNEUROSCI.1091-13.2013 (URL: http://www.jneurosci.org/content/33/27/11239, cited by 0001).

DeFelipe, J., 1993. Neocortical neuronal diversity: chemical heterogeneity revealed by colocalization studies of classic neurotransmitters, neuropeptides, calcium-binding proteins, and cell surface molecules. Cereb. Cortex 3, 273–289. http://dx.doi.org/10.1093/cercor/3.4.273 (URL: http://cercor.oxfordjournals.org/content/3/4/273, PMID: 8104567).

Destexhe, A., Mainen, Z.F., Sejnowski, T.J., 1998. Kinetic models of synaptic transmission, Methods in Neuronal Modeling, 2nd edition. MIT Press, Cambridge, MA, USA, pp. 1–26.

Ermentrout, B., Pascal, M., Gutkin, B., 2001. The effects of spike frequency adaptation and negative feedback on the synchronization of neural oscillators. Neural Comput. 13 (6), 1285–1310. http://dx.doi.org/10.1162/08997660152002861.

Fox, M.D., Snyder, A.Z., Vincent, J.L., Corbetta, M., Van Essen, D.C., Raichle, M.E., 2005. The human brain is intrinsically organized into dynamic, anticorrelated functional networks. Proc. Natl. Acad. Sci. U. S. A. 102, 9673–9678. http://dx.doi.org/10.1073/pnas.0504136102 (PMID: 15976020 PMCID: 1157105).

Fransson, P., 2005. Spontaneous low-frequency BOLD signal fluctuations: an fMRI investigation of the resting-state default mode of brain function hypothesis. Hum. Brain Mapp. 26, 15–29. http://dx.doi.org/10.1002/hbm.20113 (URL: http://onlinelibrary.wiley.com/doi/10.1002/hbm.20113/abstract).

Freyer, F., Aquino, K., Robinson, P.A., Ritter, P., Breakspear, M., 2009. Bistability and non-Gaussian fluctuations in spontaneous cortical activity. J. Neurosci. 29, 8512–8524. http://dx.doi.org/10.1523/JNEUROSCI.0754-09.2009 (URL: http://www.jneurosci.org/content/29/26/8512.abstract).

Freyer, F., Roberts, J.A., Becker, R., Robinson, P.A., Ritter, P., Breakspear, M., 2011. Biophysical mechanisms of multistability in resting-state cortical rhythms. J. Neurosci. 31,

6353–6361. http://dx.doi.org/10.1523/JNEUROSCI.6693-10.2011 (URL: http://www.jneurosci.org/content/31/17/6353).
Freyer, F., Roberts, J.A., Ritter, P., Breakspear, M., 2012. A canonical model of multistability and scale-invariance in biological systems. PLoS Comput. Biol. 8, e1002634. http://dx.doi.org/10.1371/journal.pcbi.1002634.
Fuhrmann, G., Markram, H., Tsodyks, M., 2002. Spike frequency adaptation and neocortical rhythms. J. Neurophysiol. 88, 761–770 (URL: http://jn.physiology.org/content/88/2/761.abstract).
Ghosh, A., Rho, Y., McIntosh, A.R., Kötter, R., Jirsa, V.K., 2008a. Cortical network dynamics with time delays reveals functional connectivity in the resting brain. Cogn. Neurodyn. 2, 115–120. http://dx.doi.org/10.1007/s11571-008-9044-2 (PMID: 19003478 PMCID: PMC2427063).
Ghosh, A., Rho, Y.A., McIntosh, A.R., Kötter, R., Jirsa, V.K., 2008b. Noise during rest enables the exploration of the brain's dynamic repertoire. PLoS Comput. Biol. 4, e1000196. http://dx.doi.org/10.1371/journal.pcbi.1000196.
Gong, G., He, Y., Concha, L., Lebel, C., Gross, D.W., Evans, A.C., Beaulieu, C., 2009. Mapping anatomical connectivity patterns of human cerebral cortex using in vivo diffusion tensor imaging tractography. Cereb. Cortex 19, 524–536. http://dx.doi.org/10.1093/cercor/bhn102 (URL: http://cercor.oxfordjournals.org/content/19/3/524).
Greicius, M.D., Krasnow, B., Reiss, A.L., Menon, V., 2003. Functional connectivity in the resting brain: a network analysis of the default mode hypothesis. Proc. Natl. Acad. Sci. U. S. A. 100, 253–258. http://dx.doi.org/10.1073/pnas.0135058100 (URL: http://www.ncbi.nlm.nih.gov/pubmed/12506194. PMID: 12506194).
Gusnard, D.A., Raichle, M.E., 2001. Searching for a baseline: functional imaging and the resting human brain. Nat. Rev. Neurosci. 2, 685–694. http://dx.doi.org/10.1038/35094500 (URL: http://www.nature.com/nrn/journal/v2/n10/full/nrn1001-685a.html).
Hagmann, P., Cammoun, L., Gigandet, X., Meuli, R., Honey, C.J., Wedeen, V.J., Sporns, O., 2008. Mapping the structural core of human cerebral cortex. PLoS Biol. 6, e159. http://dx.doi.org/10.1371/journal.pbio.0060159.
Helmchen, F., Imoto, K., Sakmann, B., 1996. Ca2+ buffering and action potential-evoked ca2+ signaling in dendrites of pyramidal neurons. Biophys. J. 70, 1069–1081 (PMID: 8789126 PMCID: 1225009).
Hill, S., Tononi, G., 2005. Modeling sleep and wakefulness in the thalamocortical system. J. Neurophysiol. 93, 1671–1698. http://dx.doi.org/10.1152/jn.764 00915.2004 (URL: http://jn.physiology.org/content/93/3/1671.abstract).
Hipp, J.F., Hawellek, D.J., Corbetta, M., Siegel, M., Engel, A.K., 2012. Large-scale cortical correlation structure of spontaneous oscillatory activity. Nat. Neurosci. http://dx.doi.org/10.1038/nn.3101 (URL: http://www.nature.com/neuro/journal/vaop/ncurrent/full/nn.3101.html).
Honey, C.J., Kötter, R., Breakspear, M., Sporns, O., 2007. Network structure of cerebral cortex shapes functional connectivity on multiple time scales. Proc. Natl. Acad. Sci. U. S. A. 104, 10240–10245. http://dx.doi.org/10.1073/pnas.0701519104 (URL: http://www.pnas.org/content/104/24/10240.abstract).
Honey, C.J., Sporns, O., Cammoun, L., Gigandet, X., Thiran, J.P., Meuli, R., Hagmann, P., 2009. Predicting human resting-state functional connectivity from structural connectivity. Proc. Natl. Acad. Sci. U. S. A. 106, 2035–2040. http://dx.doi.org/10.1073/pnas.0811168106 (URL: http://www.pnas.org/content/106/6/2035.abstract).
Honey, C.J., Thivierge, J.P., Sporns, O., 2010. Can structure predict function in the human brain? NeuroImage 52, 766–776. http://dx.doi.org/10.1016/j.neuroimage.2010.01.071 (URL: http://www.sciencedirect.com/science/article/pii/S1053811910000935).
Huang, M.X., Mosher, J.C., Leahy, R.M., 1999. A sensor-weighted overlapping-sphere head model and exhaustive head model comparison for MEG. Phys. Med. Biol. 44, 423–440 (PMID: 10070792).
Izhikevich, E.M., Edelman, G.M., 2008. Large-scale model of mammalian thalamocortical systems. Proc. Natl. Acad. Sci. U. S. A. 105, 3593–3598. http://dx.doi.org/10.1073/pnas.0712231105 (URL: http://www.pnas.org/content/105/9/3593).
Jenkinson, M., Bannister, P., Brady, M., Smith, S., 2002. Improved optimization for the robust and accurate linear registration and motion correction of brain images. NeuroImage 17, 825–841 (PMID: 12377157).
Jirsa, V.K., 2009. Neural field dynamics with local and global connectivity and time delay. Philos. Trans. A Math. Phys. Eng. Sci. 367, 1131–1143. http://dx.doi.org/10.1098/rsta.2008.0260 (URL: http://rsta.royalsocietypublishing.org/content/367/1891/1131).
Jirsa, V.K., Ding, M., 2004. Will a large complex system with time delays be stable? Phys. Rev. Lett. 93, 070602. http://dx.doi.org/10.1103/PhysRevLett.93.070602 (URL: http://link.aps.org/doi/10.1103/PhysRevLett.93.070602).
Knock, S., McIntosh, A., Sporns, O., Kötter, R., Hagmann, P., Jirsa, V., 2009. The effects of physiologically plausible connectivity structure on local and global dynamics in large scale brain models. J. Neurosci. Methods 183, 86–94. http://dx.doi.org/10.1016/j.jneumeth.2009.07.007 (URL: http://www.sciencedirect.com/science/article/pii/S0165027009003707).
Liu, Y.H., Wang, X.J., 2001. Spike-frequency adaptation of a generalized leaky integrate-and-fire model neuron. J. Comput. Neurosci. 10, 25–45 (URL: http://www.ncbi.nlm.nih.gov/pubmed/11316338. PMID: 11316338).
Liu, Z., Fukunaga, M., de Zwart, J.A., Duyn, J.H., 2010. Large-scale spontaneous fluctuations and correlations in brain electrical activity observed with magnetoencephalography. NeuroImage 51, 102–111. http://dx.doi.org/10.1016/j.neuroimage.2010.01.092 (PMID: 20123024 PMCID: 2847019).
Llinas, R.R., 1988. The intrinsic electrophysiological properties of mammalian neurons: Insights into central nervous system function. Science 242, 1654–1664. http://dx.doi.org/10.1126/science.3059497 (URL: http://www.sciencemag.org/content/242/4886/1654).
Lopes da Silva, F.H., Hoeks, A., Smits, H., Zetterberg, L.H., 1974. Model of brain rhythmic activity. The alpha-rhythm of the thalamus. Kybernetik 15, 27–37 (URL: http://www.ncbi.nlm.nih.gov/pubmed/4853232. PMID: 4853232).
Lowe, M., Mock, B., Sorenson, J., 1998. Functional connectivity in single and multislice echoplanar imaging using resting-state fluctuations. NeuroImage 7, 119–132. http://dx.doi.org/10.1006/nimg.1997.0315 (URL: http://www.sciencedirect.com/science/article/pii/S1053811997903153).
Luckhoo, H., Hale, J.R., Stokes, M.G., Nobre, A.C., Morris, P.G., Brookes, M.J., Woolrich, M.W., 2012. Inferring task-related networks using independent component analysis in magnetoencephalography. NeuroImage 62, 530–541. http://dx.doi.org/10.1016/j.neuroimage.2012.04.046 (PMID: 22569064).
Magee, J.C., 2000. Dendritic integration of excitatory synaptic input. Nat. Rev. Neurosci. 1, 181–190. http://dx.doi.org/10.1038/35044552 (URL: http://www.nature.com/nrn/journal/v1/n3/full/nrn1200_181a.html).
Mantini, D., Perrucci, M.G., Del Gratta, C., Romani, G.L., Corbetta, M., 2007. Electrophysiological signatures of resting state networks in the human brain. Proc. Natl. Acad. Sci. U. S. A. 104, 13170–13175. http://dx.doi.org/10.1073/pnas.0700668104 (URL: http://www.pnas.org/content/104/32/13170.abstract).
Mazoyer, B., Zago, L., Mellet, E., Bricogne, S., Etard, O., Houdé, O., Crivello, F., Joliot, M., Petit, L., Tzourio-Mazoyer, N., 2001. Cortical networks for working memory and executive functions sustain the conscious resting state in man. Brain Res. Bull. 54, 287–298. http://dx.doi.org/10.1016/S0361-9230(00)00437-8 (URL: http://www.sciencedirect.com/science/article/pii/S0361923000004378).
Mazzoni, A., Panzeri, S., Logothetis, N.K., Brunel, N., 2008. Encoding of naturalistic stimuli by local field potential spectra in networks of excitatory and inhibitory neurons. PLoS Comput. Biol. 4, e1000239. http://dx.doi.org/10.1371/journal.pcbi.1000239.
Meech, R.W., 1978. Calcium-dependent potassium activation in nervous tissues. Annu. Rev. Biophys. Bioeng. 7, 1–18. http://dx.doi.org/10.1146/annurev.bb.07.060178.000245 (URL: http://www.annualreviews.org/doi/abs/10.1146/annurev.bb.07.060178.000245).
Neymotin, S.A., Lee, H., Park, E., Fenton, A.A., Lytton, W.W., 2011. Emergence of physiological oscillation frequencies in a computer model of neocortex. Front. Comput. Neurosci. 5, 19. http://dx.doi.org/10.3389/fncom.2011.00019 (URL: http://www.ncbi.nlm.nih.gov/pubmed/21541305. PMID: 21541305).
Sarter, M., Bruno, J., 1999. Cortical cholinergic inputs mediating arousal, attentional processing and dreaming: differential afferent regulation of the basal forebrain by telencephalic and brainstem afferents. Neuroscience 95, 933–952. http://dx.doi.org/10.1016/S0306-4522(99)00487-X (URL: http://www.sciencedirect.com/science/article/pii/S030645229900487X).
Senden, M., Goebel, R., Deco, G., 2012. Structural connectivity allows for multi-threading during rest: the structure of the cortex leads to efficient alternation between resting state exploratory behavior and default mode processing. NeuroImage 60, 2274–2284. http://dx.doi.org/10.1016/j.neuroimage.2012.02.061 (URL: http://www.sciencedirect.com/science/article/pii/S105381191200239X).
Shaw, J.C., 2003. The Brain's Alpha Rhythms and the Mind: a Review of Classical and Modern Studies of the Alpha Rhythm Component of the Electroencephalogram with Commentaries on Associated Neuroscience and Neuropsychology. Elsevier Health Sciences.
Silva, L., Amitai, Y., Connors, B., 1991. Intrinsic oscillations of neocortex generated by layer 5 pyramidal neurons. Science 251, 432–435. http://dx.doi.org/10.1126/science.1824881 (URL: http://www.sciencemag.org/content/251/4992/432.abstract).
Spiegler, A., Jirsa, V., 2013. Systematic approximations of neural fields through networks of neural masses in the virtual brain. Neuroimage 83C, 704–725. http://dx.doi.org/10.1016/j.neuroimage.2013.06.018 (cited by 0000).
Steriade, M., 1997. Synchronized activities of coupled oscillators in the cerebral cortex and thalamus at different levels of vigilance. Cereb. Cortex 7, 583–604 (Cited by 0302).
Stiefel, K.M., Gutkin, B.S., Sejnowski, T.J., 2009. The effects of cholinergic neuromodulation on neuronal phase-response curves of modeled cortical neurons. J. Comput. Neurosci. 26, 289–301. http://dx.doi.org/10.1007/s10827-008-0111-9 (URL: http://www.ncbi.nlm.nih.gov/pmc/articles/PMC2857973/, cited by 0034).
Svoboda, K., Denk, W., Kleinfeld, D., Tank, D.W., 1997. In vivo dendritic calcium dynamics in neocortical pyramidal neurons. Nature 385, 161–165. http://dx.doi.org/10.1038/385161a0.
Taulu, S., Simola, J., Kajola, M., 2005. Applications of the signal space separation method. IEEE Trans. Signal Process. 53, 3359–3372. http://dx.doi.org/10.1109/TSP.2005.853302.
Tzourio-Mazoyer, N., Landeau, B., Papathanassiou, D., Crivello, F., Etard, O., Delcroix, N., Mazoyer, B., Joliot, M., 2002. Automated anatomical labeling of activations in SPM using a macroscopic anatomical parcellation of the MNI MRI single-subject brain. NeuroImage 15, 273–289. http://dx.doi.org/10.1006/nimg.2001.0978 (URL: http://www.sciencedirect.com/science/article/pii/S1053811901909784).
van den Heuvel, M.P., Mandl, R., Hulshoff Pol, H., 2008. Normalized cut group clustering of resting-state fMRI data. PLoS One 3, e2001. http://dx.doi.org/10.1371/journal.pone.0002001.
Van Essen, D.C., Glasser, M.F., Dierker, D.L., Harwell, J., Coalson, T., 2012. Parcellations and hemispheric asymmetries of human cerebral cortex analyzed on surface-based atlases. Cereb. Cortex 22, 2241–2262. http://dx.doi.org/10.1093/cercor/bhr291. cited by 0035.
Vazquez, J., Baghdoyan, H.A., 2001. Basal forebrain acetylcholine release during REM sleep is significantly greater than during waking. Am. J. Physiol. Regul. Integr. Comp. Physiol. 280, R598–R601 (URL: http://ajpregu.physiology.org/content/280/2/R598. PMID: 11208592).
Wang, J., Wang, L., Zang, Y., Yang, H., Tang, H., Gong, Q., Chen, Z., Zhu, C., He, Y., 2009. Parcellation-dependent small-world brain functional networks: a resting-state fMRI study. Hum. Brain Mapp. 30, 1511–1523. http://dx.doi.org/10.1002/hbm.20623 (URL: http://onlinelibrary.wiley.com/doi/10.1002/hbm.20623/abstract).
Zalesky, A., Fornito, A., Harding, I.H., Cocchi, L., Yücel, M., Pantelis, C., Bullmore, E.T., 2010. Whole-brain anatomical networks: does the choice of nodes matter? NeuroImage 50,

970–983. http://dx.doi.org/10.1016/j.neuroimage.2009.12.027 (URL: http://www.sciencedirect.com/science/article/pii/S1053811909013159).
Zimmerman, D.W., Zumbo, B.D., Williams, R.H., 2003. Bias in estimation and hypothesis testing of correlation. Psicológica (001). Retrieved from http://redalyc.uaemex.mx/src/inicio/ArtPdfRed.jsp?iCve=16924109.
Zhu, Z., Zumer, J.M., Lowenthal, M.E., Padberg, J., Recanzone, G.H., Krubitzer, L.A., Nagarajan, S.S., Disbrow, E.A., 2009. The relationship between magnetic and electrophysiological responses to complex tactile stimuli. BMC Neurosci. 10, 4. http://dx.doi.org/10.1186/1471-2202-10-4 (PMID: 19146670 PMCID: 2652466).